PERGAMON

International Journal of Heat and Mass Transfer 42 (1999) 1645–1664

International Journal of HEAT and MASS TRANSFER

Large scale motions in a manipulated turbulent boundary layer

N. Rashidnia[a], A.B. Ebiana[b,*]

[a] *NCMR Inc., NASA Lewis Research Center, Brook Park, OH 44142, U.S.A.*
[b] *Mechanical Engineering Department, Cleveland State University, Cleveland, OH 44115, U.S.A*

Received 23 July 1998

Abstract

Experiments were performed to examine structural changes that exist in a turbulent boundary layer with measured 2–10% net drag reduction obtained using a tandem arranged parallel plate manipulator (hereafter abbreviated TAPPM). Conditionally sampled and space-time correlation measurements support a picture of approximately equal reductions in the streamwise and normal components of the large scale fluctuations, both in the boundary layer and in the irrotational ambient flow in the valleys between the large scale motions (LSMs) at $20\delta_o$. However, by $51\delta_o$, both the LSMs and the response of the irrotational ambient flow relax to approximately their unmanipulated state. Simple modeling suggests that in the valleys of irrotational fluid the motion would reestablish itself in 5δ, and it is suggested that the presence of the TAPPM's wake in the outer region inhibits the reformation of these large scale wallward sweeps sustaining the lower values of the local skin friction, C_f. Because of the thick boundary layer in the present experiment, at $20\delta_o$ the TAPPM's wake has not entered the wall region, in contrast to many other investigations. At streamwise locations just before the main body of the wake intersects the wall ($56\delta_o$), a rapid rise in C_f is observed. Afterwards, a small reduction in C_f (confirmed by three independent methods of measurements) is maintained resulting from the remaining defect in the wake, which lasts until the wake is fully mixed.

Nomenclature

C_f local skin friction
C_{fc} local skin friction obtained from Clauser plots
C_{fn} local skin friction obtained from wall slope measurements
C_{fp} local skin friction obtained from Preston tube
$C_{f\theta}$ local skin friction obtained from momentum balance
$R_{u1'u2'}$ correlation of the large scale streamwise fluctuations
$R_{v1'v2'}$ correlation of the large scale normal fluctuations
$R_{u1'v2'}$ cross correlation of the large scale streamwise and normal fluctuations
u_τ friction velocity
u' fluctuating u-component velocity
v' fluctuating v-component velocity
$u'v'$ product of fluctuating u- and v-component velocities
U_∞ free stream velocity
x, y, z 3-D Cartesian coordinate directions
x_o x-location of the TAPPM from the leading edge of the test wall.

Greek symbols
$\langle\ \rangle$ averaged quantity
δ boundary layer thickness
δ_o boundary layer thickness at the upstream plate of the TAPPM
v kinematic viscosity
$\xi = (x - x_o)/\delta_o$ non-dimensional x-coordinate direction
$\tau = \Delta t \cdot U_\infty/\delta$ shear stress.

Abbreviations
LEBU large eddy breakup device
LSM large scale motion
TAPPM tandem arranged parallel plate manipulator

* Corresponding author. Tel.: 001 216 687 5276; fax: 001 216 687 5375; e-mail: ebiana@csvax.csuohoi.edu

0017–9310/98/$ - see front matter
PII: S0017–9310(98)00219–1

1. Introduction

It is now well known that a tandem arranged parallel plate manipulator (TAPPM) can produce a net drag reduction in turbulent boundary layers [1–11]. However, the physical changes produced by the TAPPM are the concerns of this research, and need elucidation to extrapolate potential applications in aircraft and other technological applications. Although at an early stage of our knowledge the acronym LEBU (Large Eddy Breakup Device) was used to describe their effect, there have not, to our knowledge, been a series of measurements in which the flow field and Reynolds stress of the large eddies were measured when devices that actually gave drag reduction were in place. In addition, a number of investigators [6, 7, 12–14] have noted that the wake may play an important part in the dynamics of the flow. The possible effects of a TAPPM have been divided into 'plate' and 'wake' effects [13–14]. The wake effects are expected to persist for greater distances than the plate effects and be responsible for sustaining C_f reductions long enough to overcome device drag and result in net drag reduction. Among the 'wake' effects are shielding [12], wake/sublayer interactions [6], wake defect [15], vortex unwinding [16–17], and blocking [18]. Although all these are probably active, determining which play a dominant role is essential to our further understanding and optimization of our layer manipulation.

It has been suggested that the dissipative eddies in the wake acted as a 'shield' which dissipated energy from wallward moving high speed fluid, and thus inhibited the reestablishment of the large scale wallward sweeps of high speed irrotational fluid which are an important part of the turbulence production process [9–10, 12]. A similar effect, but one that inhibits the transport of energy from the inertial range of the spectrum, in the log region to the sublayer, called blocking has been proposed by Choi [18]. Savill and Mumford [6] discussed the possibility that coherent motions in the wake could interact with the wall region flow to inhibit the production of turbulence. Taylor [15] suggested that the relatively large defect in the TAPPM wakes, relative to the boundary layer effect, would produce lower skin friction because the defect would be transported by the turbulence, in both the wake and the boundary layer, to the wall region. This hypothesis does not require any change in the transport properties of the boundary layer, in particular, it does not require the ability of turbulent mixing in the boundary layer to decelerate fluid. Bushnell [16] and also Sreenivasan and Narasimha [13] suggested that the trailing vorticity from the plates due to the unsteady circulation induced by the passage of a LSM has the opposite sign to that of the rotation in the LSM, thus unwinding it. Among the other unsolved puzzles is why the TAPPM results in lower skin friction reduction than a single plate of combined same total length in the flow direction, when the single plate has lower drag than the TAPPM [2, 6]. We will present data that allows us to attempt to separate the wake effects and address the importance of these mechanisms. To this end, a flow was established in which we could measure the net drag reduction using both a momentum balance and a skin friction and device drag estimate. A net drag reduction of 10% was measured using the momentum balance. Estimates from the local skin friction measurement and device drag, in the same flow, were 2%. These have been discussed elsewhere [8], but we can conclude that the TAPPM produced a net drag reduction. At $20\delta_o$ simultaneous laser sheet flow visualization and hot-wire anemometry were used to enable us to conditionally sample the u', v', and $u'v'$ information of the large eddies in both manipulated and normal boundary layers, and obtain ensemble averages. The probes used (see Fig. 3a) were two x-wires located at $y/\delta = 0.4$ and 0.6 (the TAPPM was located at $0.8\delta_o$ as shown in Fig. 1). To gain an understanding of the wake effects, flow visualization using $TiCl_4$ to mark the plate wakes was performed. Changes in the wall region transport averaged over $\pm 3.3\delta$ around $20\delta_o$ were measured by following the envelop of $TiCl_4$ that rose from the marked area of the wall. Simultaneous visualization from both surfaces provided information on the interactions. Furthermore, spatially separated temporal correlations of u, v and uv from the two x-wires were obtained at both $20\delta_o$ and at $51\delta_o$, with the wires separated by 0.5δ in the stream direction and 0.2δ normal to the wall. The technique, pioneered by Kovasznay et al. [19], yields information on the LSMs, and thus, will give some indication of the effect of the TAPPM on the LSMs. We chose to measure the frequency of occurrence of the bursting process using flow visualization from a sublayer slit [12] at $51\delta_o$, where we obtained our maximum skin friction reduction (40%) using the momentum balance; however at this location Preston tube, Clauser plot and wall slope estimates indicated only 5% reductions. Additionally, the thick boundary layer developed for this experiment allowed sublayer thickness to be measured using hot-wire anemometry. All of these measurements were compared with the unmanipulated flow in the same flow.

2. Experiments performed

The differences in skin friction and net drag reduction were measured in three ways; using a momentum balance, Preston tube and local skin friction measurements combined with an estimate of the drag of the manipulator. The skin friction obtained from the momentum balance is denoted $C_{f\theta}$, that from the local wall slope measurements C_{fn} which closely relate to C_{fc} using Clauser plots and C_{fp} was measured using Preston tube [8] in spanwise direction at several locations along the test plate. The results of absolute C_{fn} measurements using hot-wires

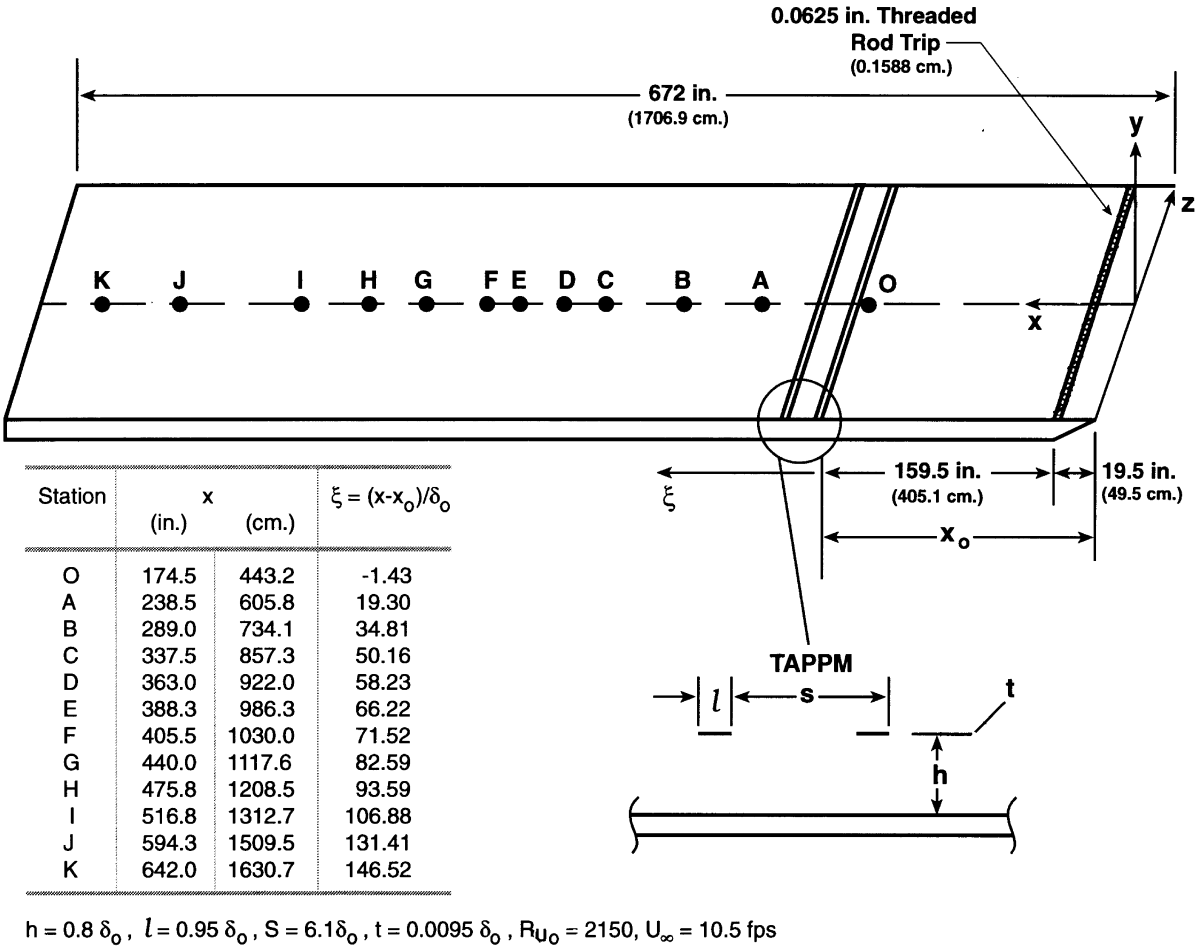

Station	x (in.)	x (cm.)	$\xi = (x-x_o)/\delta_o$
O	174.5	443.2	-1.43
A	238.5	605.8	19.30
B	289.0	734.1	34.81
C	337.5	857.3	50.16
D	363.0	922.0	58.23
E	388.3	986.3	66.22
F	405.5	1030.0	71.52
G	440.0	1117.6	82.59
H	475.8	1208.5	93.59
I	516.8	1312.7	106.88
J	594.3	1509.5	131.41
K	642.0	1630.7	146.52

$h = 0.8\,\delta_o$, $l = 0.95\,\delta_o$, $S = 6.1\delta_o$, $t = 0.0095\,\delta_o$, $Re_{\delta_o} = 2150$, $U_\infty = 10.5$ fps

Fig. 1. The tandem arranged parallel plate manipulator (TAPPM).

appear to be lower due to hot-wire interference effects, but use of the ratio of manipulated values normalizes out this constant effect.

Figure 1 shows the boundary layer manipulator configuration used in these experiments. The ribbon-type manipulators were parallel to the wall to within the 0.2° accuracy needed to have their drag be only approximately 10% higher than that due to the laminar skin friction on their surfaces [20].

Three types of experiments were performed to determine the changes in the LSMs: contaminant movement studies, space-time correlations and simultaneous hot-wire anemometry and flow visualization. In addition profiles of the mean velocity were measured, extending into the sublayer, enabling us to obtain the sublayer thickness, as well as C_{fn}. For purposes of comparison, independent Preston tube measurements were also made.

Passive contaminants were used to determine whether there was an appreciable change in the flux of mass from the wall region with the TAPPM, and to determine how it correlated with the spread of the TAPPM's wakes. Figure 2 shows the arrangement for our study of the spread of the wake and the liftup of wall layer fluid.

Figure 3a shows the probe arrangement for our study of the correlation at a large spatial separation. Custom made 5 μm diameter, 1 mm (active) long tungsten wires, copper plated at the ends, were combined with DISA 55M10 anemometers to make the measurements. Figure 3b shows a schematic of the moveable (in spanwise direction) Preston tube that was used for the C_{fp} measurements. More details can be found in [8].

Figure 4 shows the arrangement for the simultaneous flow visualization/hot-wire anemometry studies. The same hot-wire arrangement was used. Operating the pro-

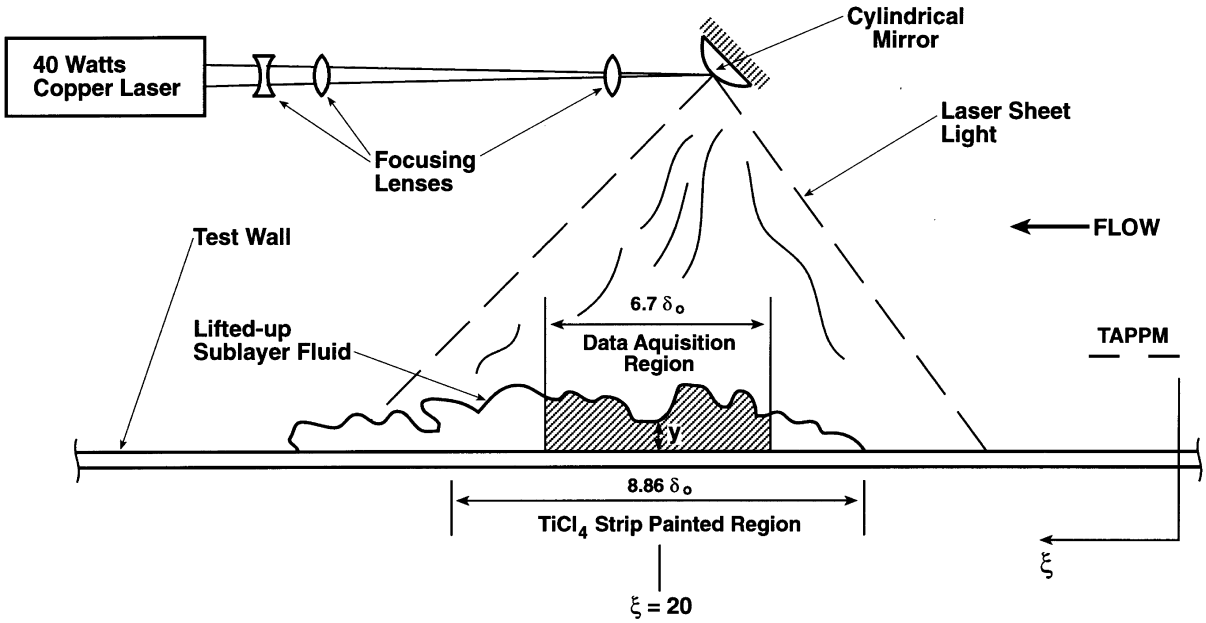

Fig. 2. The arrangement for our study of the spread of the wake and the transport of wall layer fluid.

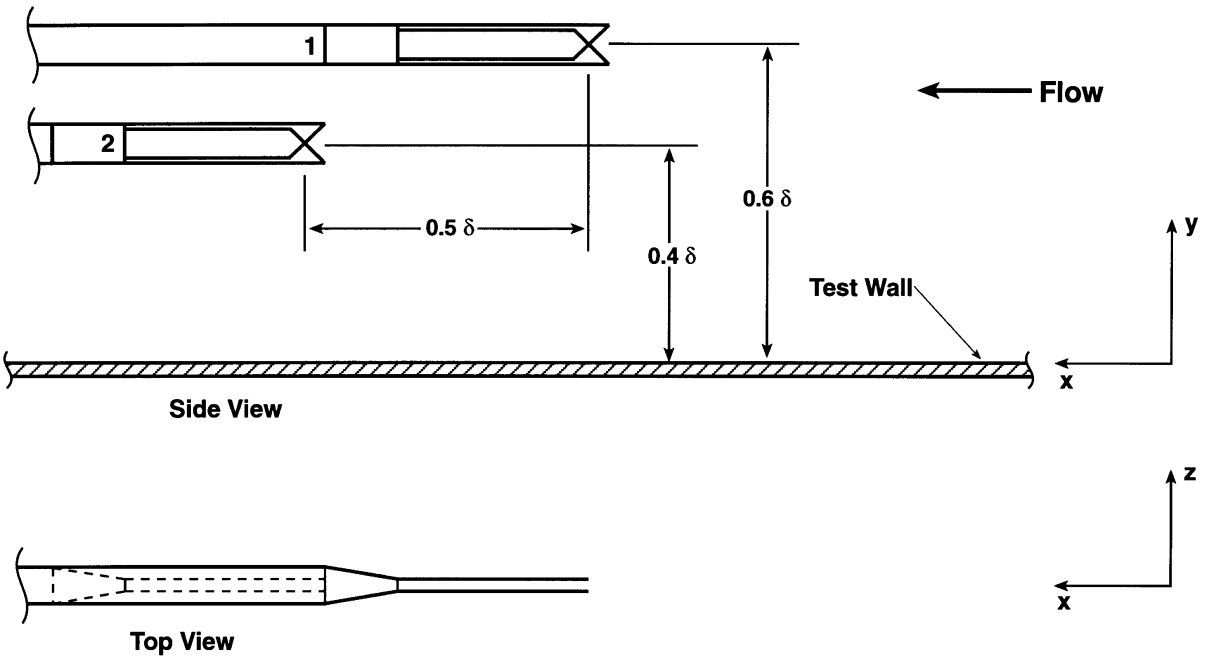

Fig. 3. (a) The probe arrangement used to obtain spatially separated temporal correlations

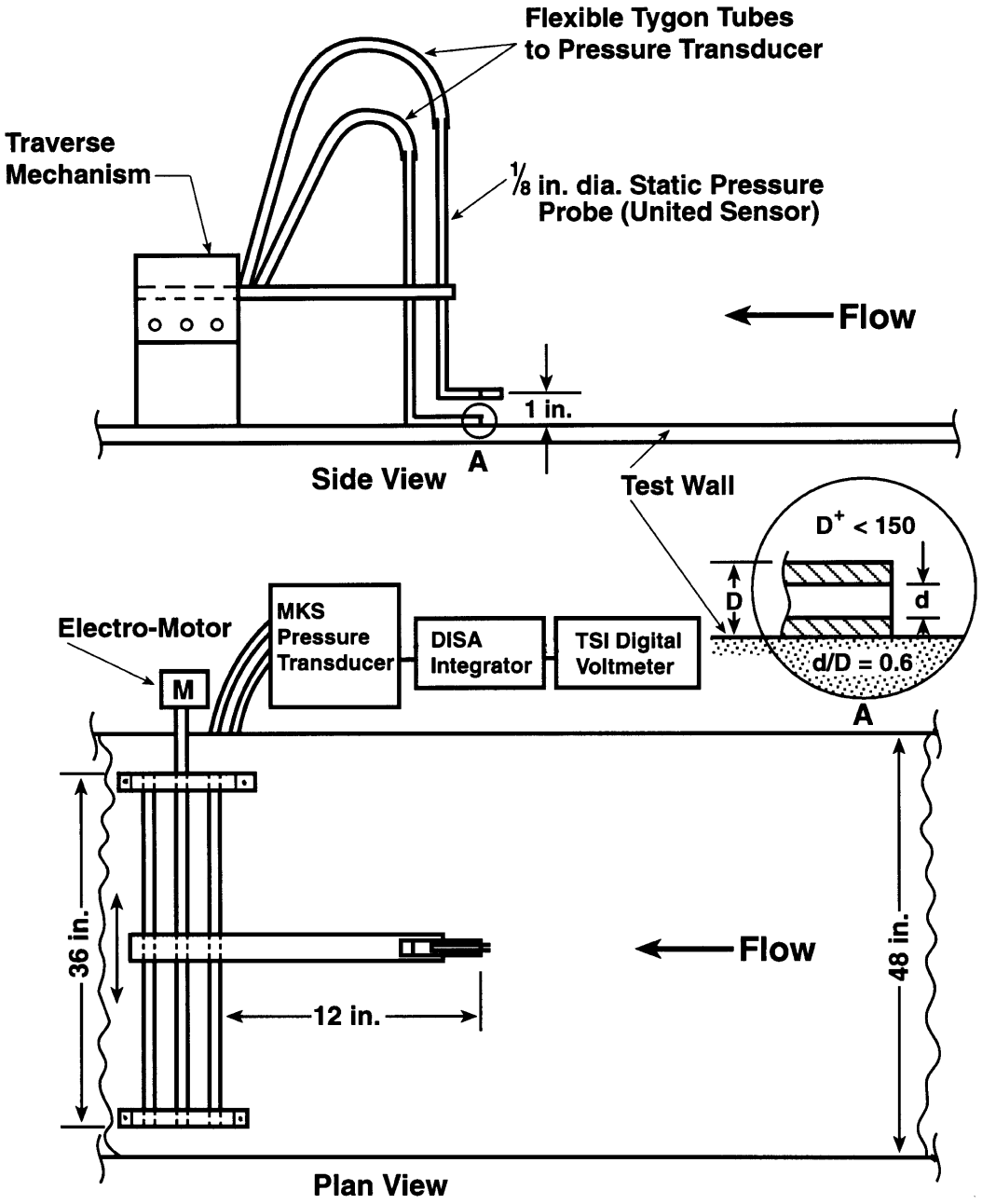

Fig. 3. (b) Schematic of the movable (modified) Preston tube probe.

bes at 1.8 resistance ratio allowed accurate results to be obtained in the oil-fog ambient [8].

3. Results

The main goal of our experiments is to understand the physics of TAPPM interactions in a flow in which the TAPPM produced net drag reduction. Figure 5a and b show the net drag reduction and the skin friction variations found using both a momentum balance, and local C_f measurements, obtained during the experimental runs. Although there is a large difference between use of the two techniques on the same data set, it is clear that we are looking at changes that occur when there is net drag reduction.

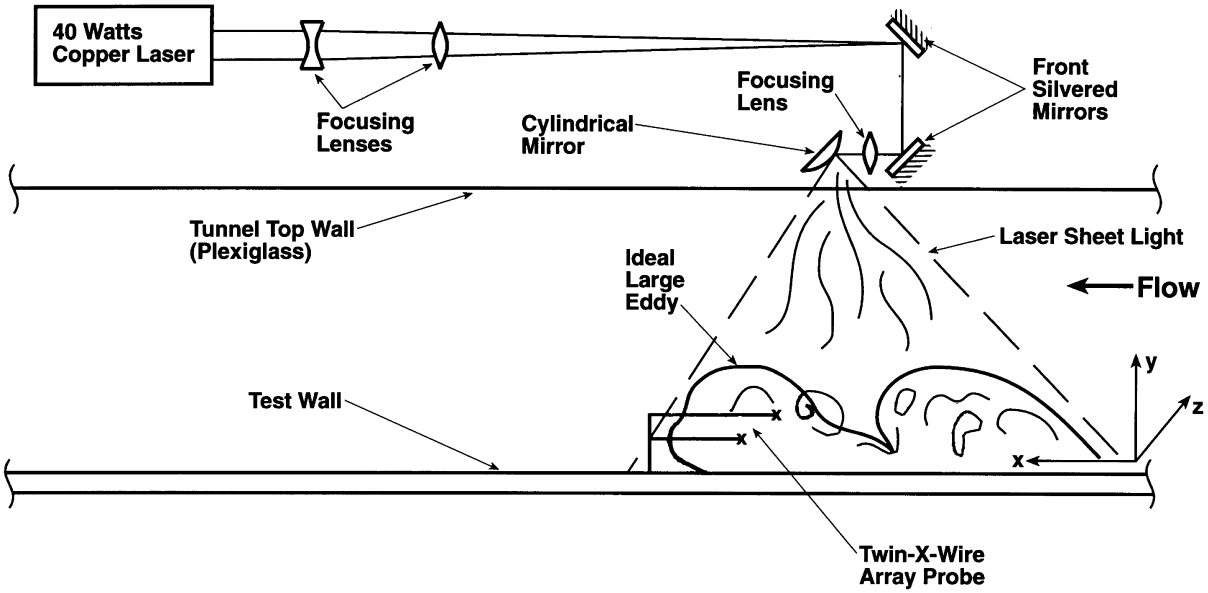

Fig. 4. Experimental arrangement used to obtain simultaneous flow visualization and hot-wire data.

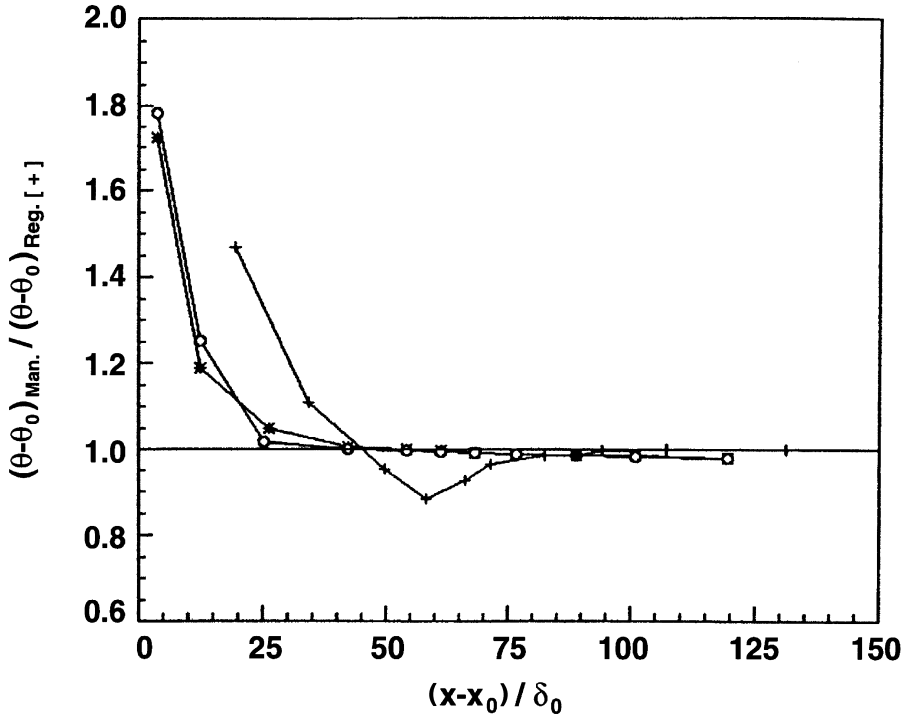

Fig. 5. (a) The net drag reduction from the TAPPM, obtained using a momentum balance [*], near wall slope measurements [+] and Preston tube measurements [o].

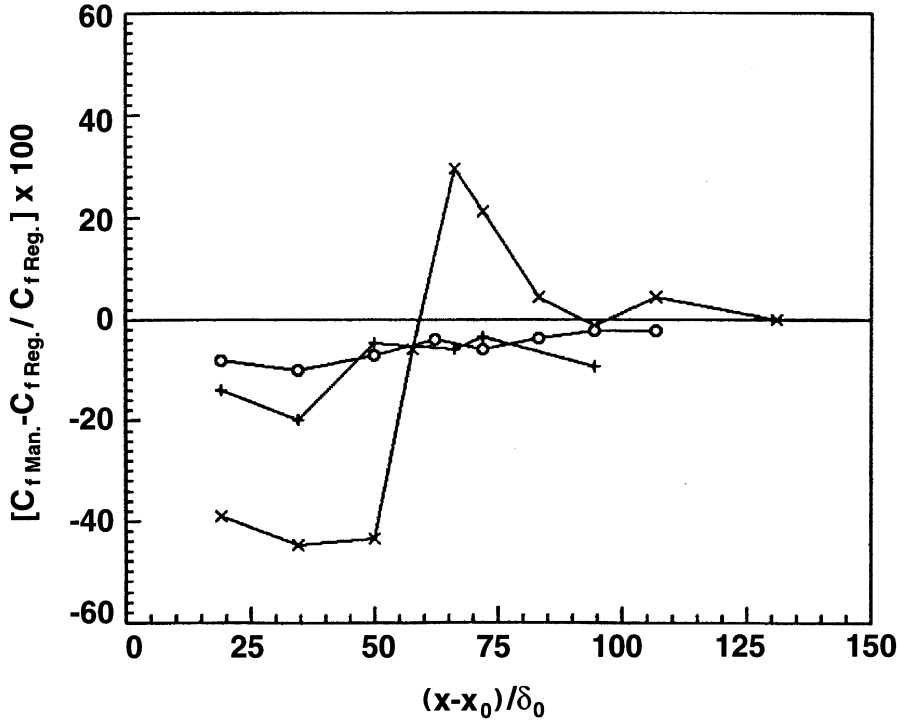

Fig. 5. (b) Skin friction changes measured using a momentum balance [*], near wall slope measurements [+] and Preston tube measurements [o].

We first present data which is representative of the large scale motions, both within the boundary layer and adjacent to it, and the changes they undergo with the TAPPM, then address the larger question of what mechanisms are largely responsible for the reduced skin friction. All large scale motion data have been non-dimensionalized using U_∞ as the relevant velocity scale. We will first discuss the changes at $\xi = 20$ ($\xi = (x - x_o)/\delta_o$) where $C_{f\theta}$ (momentum balance) is 40% lower and C_{fn} (wall slope) is 16% lower (see Fig. 5b), followed by the situation at $51\delta_o$, where we cross the break even point of drag reduction (using either method), and $C_{f\theta}$ is still $\doteq$ 40%, while both C_{fn} and C_{fp} show only 5% lower. Inspection of our laser sheet movies indicated that we could still distinguish the LSM, contrary to the visual results using smoke-wire techniques [21]. Figure 6 shows the ensemble averaged signatures of u', v' and $u'v'$ for the large scale motions with and without the TAPPMs at $y/\delta = 0.6$, $20\delta_o$ downstream. The vertical lines are the scaled LSM boundaries. Within the LSMs we see that both the streamwise fluctuation velocity and the outward moving normal fluctuation are reduced by 30%. The Reynolds stress within the LSM was even more dramatically reduced, to the point of being less than the long time average. The ensemble averaged signatures of the velocity fluctuations upstream and downstream of the LSMs were also altered. The wallward normal fluctuation velocity decreased by $\doteq$ 25% near the upstream boundary of the LSMs and by $\doteq$ 30% near the downstream boundary. The high speed streamwise fluctuation decreased by 30% at the upstream boundary, but little change was measured downstream of the averaged LSM. The Reynolds stress, which shows a weak signature in the unmanipulated boundary layer, showed no appreciable signature in the manipulated boundary layer. The magnitude of $\langle u'v' \rangle$ was reduced by 40% from the long time average value.

Figure 7 shows the ensemble averaged signatures of u', v', and $u'v'$ for the large scale motions with and without the TAPPMs at $y/\delta = 0.4$, $20\delta_o$ downstream. Within the average LSM the streamwise component was reduced $\doteq$ 30% and the normal component $\doteq$ 25%. Near the upstream boundary the high speed streamwise fluctuation was reduced by more than 50% and the wallward perturbation was reduced by 60%. The Reynolds stress at this level in the layer does not show a signature within the LSM or near its boundaries, but is reduced overall by more than 50%.

At both levels the large reduction in the Reynolds stress is further aided by the phase shift in the $\langle u' \rangle$ and $\langle v' \rangle$ signatures, with the peak in outward moving fluid shifting towards the center of the LSMs.

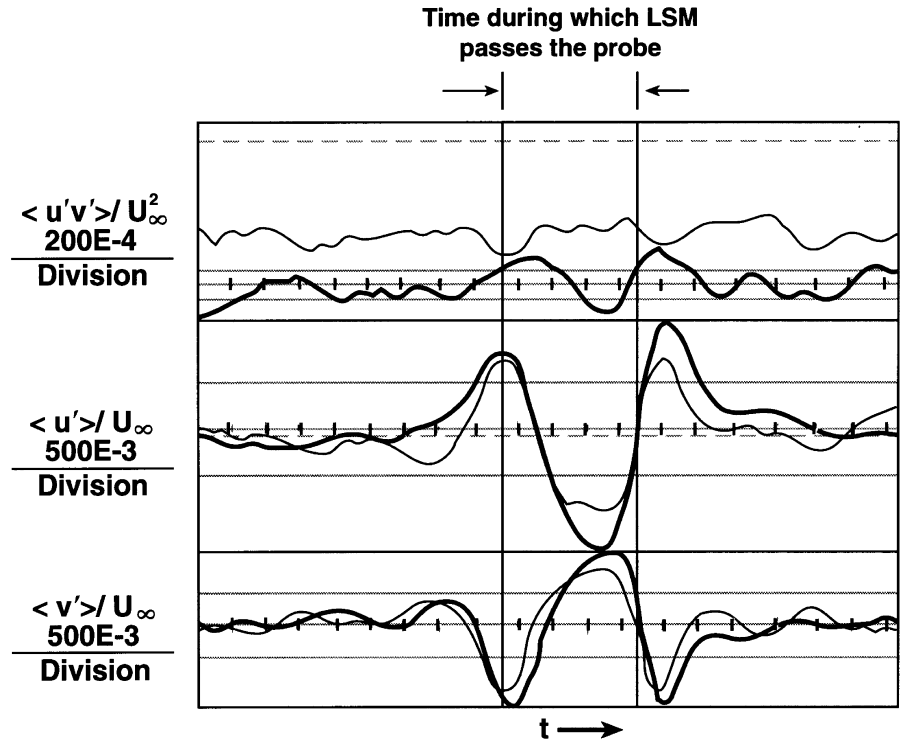

Fig. 6. Conditional sampled ensemble averaged signatures for both the TAPPM and regular flows at $y/\delta = 0.6$ and $\xi = 20$.

Results of the long time averaged spatially separated temporal correlations are shown in Figs 8–11. They are also normalized using U_∞. The correlation of the large scale normal fluctuations (Fig. 8) was reduced by 50%, and the correlation of the streamwise components (Fig. 9) was 60% lower, while that of the cross correlation of streamwise fluctuations at 0.6δ and the normal fluctuations at 0.4δ (Fig. 10) was reduced by more than 50%. The normalized correlation of the large scale components of the Reynolds stress (Fig. 11) was reduced to little more than the background level.

These results are consistent with the conditionally sampled measurements. For example, within the LSMs the 30% decrease in u' at 0.6δ and the 30% decrease in u' at 0.4δ, if it occurred in each LSM, would result in a 50% decrease in $R_{u1}u'_2$. As indicated we find a 60% decrease. Similarly, the 30% decrease in v' at 0.6δ and the 25% decrease at 0.4δ would result in a 53% decrease in $Rv'_1v'_2$; we find a 50% decrease. Thus, the changes in the spatially separated temporal correlations are indicative of changes in the motion of the large eddies.

Summarizing the probe results at $20\delta_o$, the conditionally sampled measurements show that, on average, within the LSM there is a weaker movement of low speed fluid away from the wall, and a significantly reduced large scale component of $u'v'$ when the TAPPMs were present. Furthermore, with the TAPPMs the flow in the 'valleys' is reduced, both upstream and downstream of LSMs. The integral scales obtained by integrating the area under the curves of Figs 8–11 would show a marked decrease in the respective scales, suggesting large eddy breakup. But although the large eddies in the boundary layer are significantly affected by TAPPM—as are the irrotational large scale motions that respond to them—the modifications are better described as 'decorrelated' rather than 'broken up' (which was first reported by Rashidnia [8]), because their overall flow fields are largely intact.

By using flow visualization techniques, the detail effect of these changes on the dynamics closer to the wall were studied. By painting a well defined area with $TiCl_4$, and photographing the transport of the marker away from the wall for both cases, we were able to determine the extent of TAPPM effects on transport near the wall. Figure 12 shows a histogram of the average extent that the marker was transported into the flow for both TAPPM and regular cases. The mean value of penetration in wall units, averaged over $\pm 3.3\delta_o$, shows a 25% reduction, from $y^+ = 240$ to 180, when the TAPPMs are present. This significant decrease in the distance marker was transported into the log region makes it clear that the large scale transport across the boundary layer is significantly changed by the TAPPM.

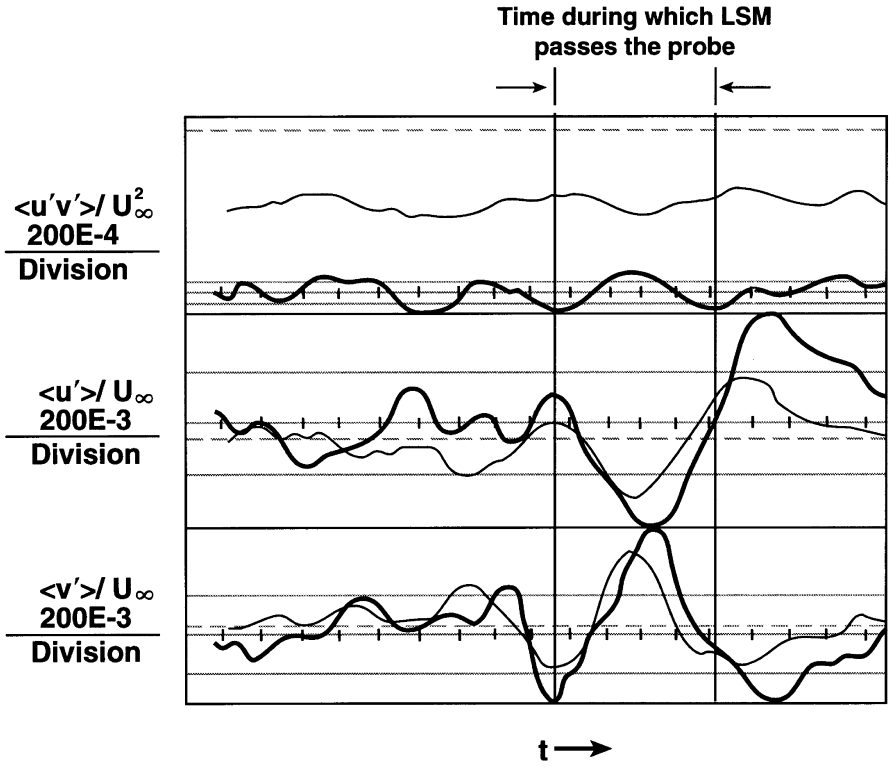

Fig. 7. Conditional sampled ensemble averaged signatures for both the TAPPM and regular flows at $y/\delta = 0.4$ and $\xi = 20$.

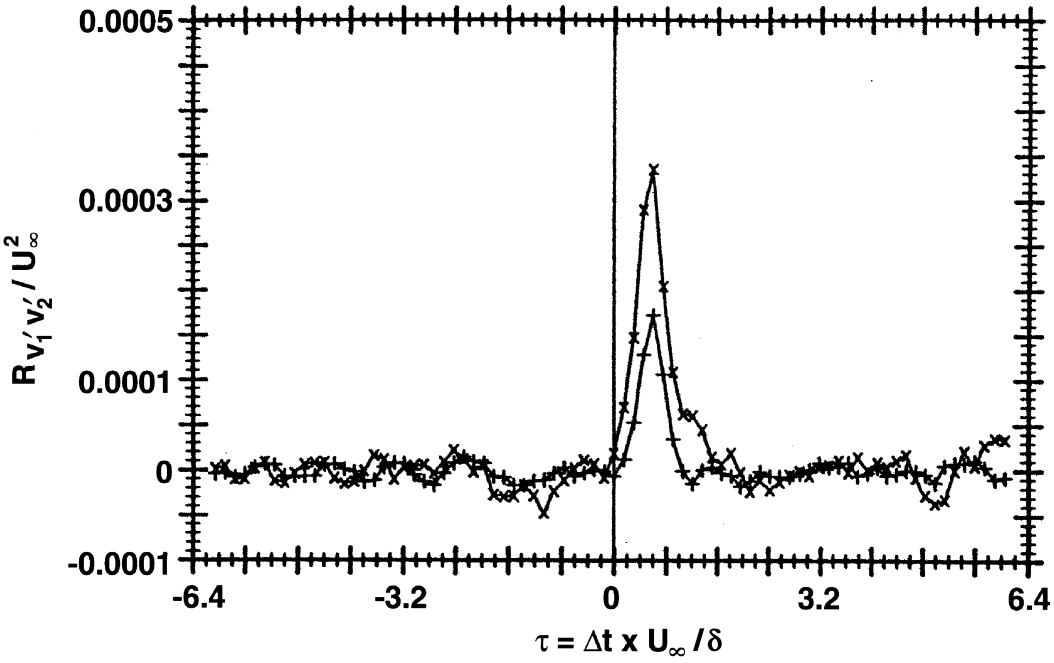

Fig. 8. Variation of $R_{v1v2'}/U_{\infty}^2$ with τ for regular (x) and TAPPMed (+) boundary layers at $\xi = 20$.

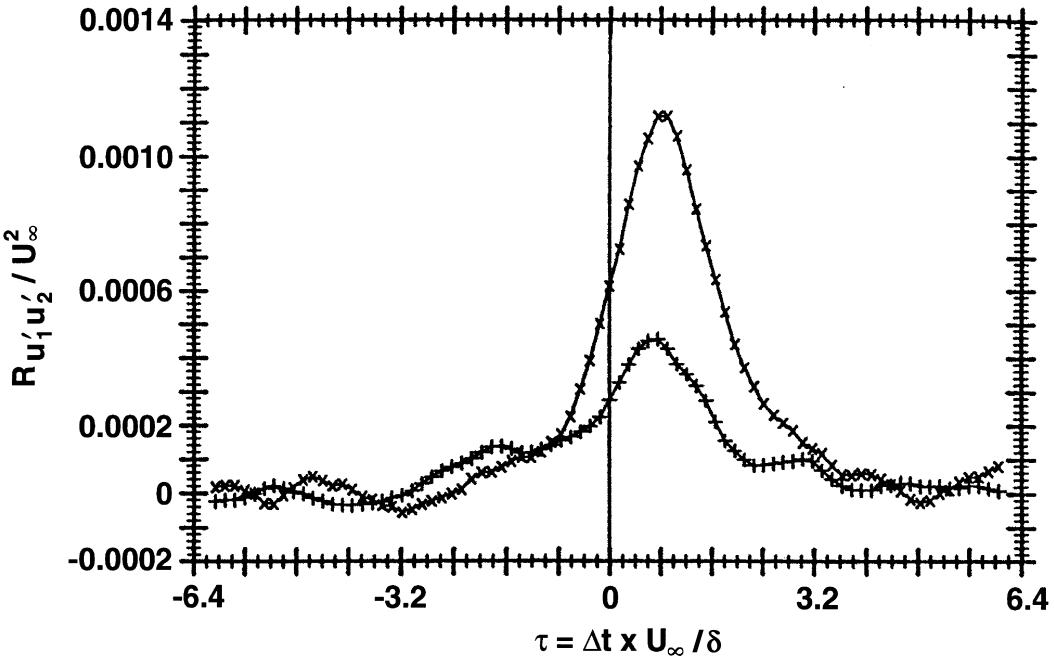

Fig. 9. Variation of $R_{u1'u2'}/U_\infty{}^2$ with τ for regular (x) and TAPPMed (+) boundary layers at $\xi = 20$.

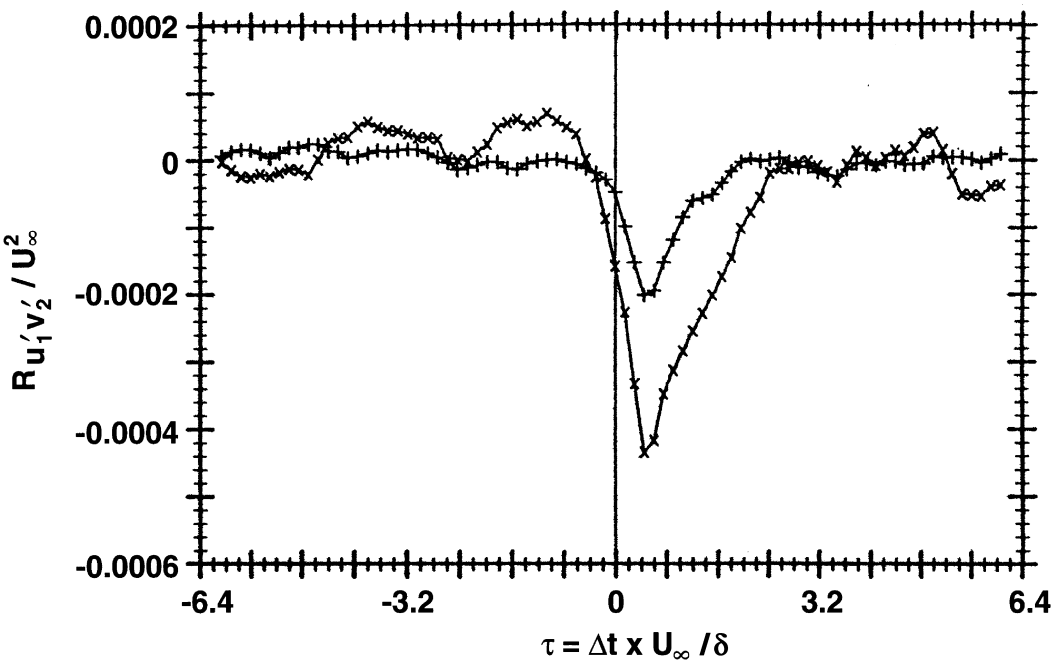

Fig. 10. Variation of $R_{u1'v2'}/U_\infty{}^2$ with τ for regular (x), and TAPPMed (+) boundary layers at $\xi = 20$.

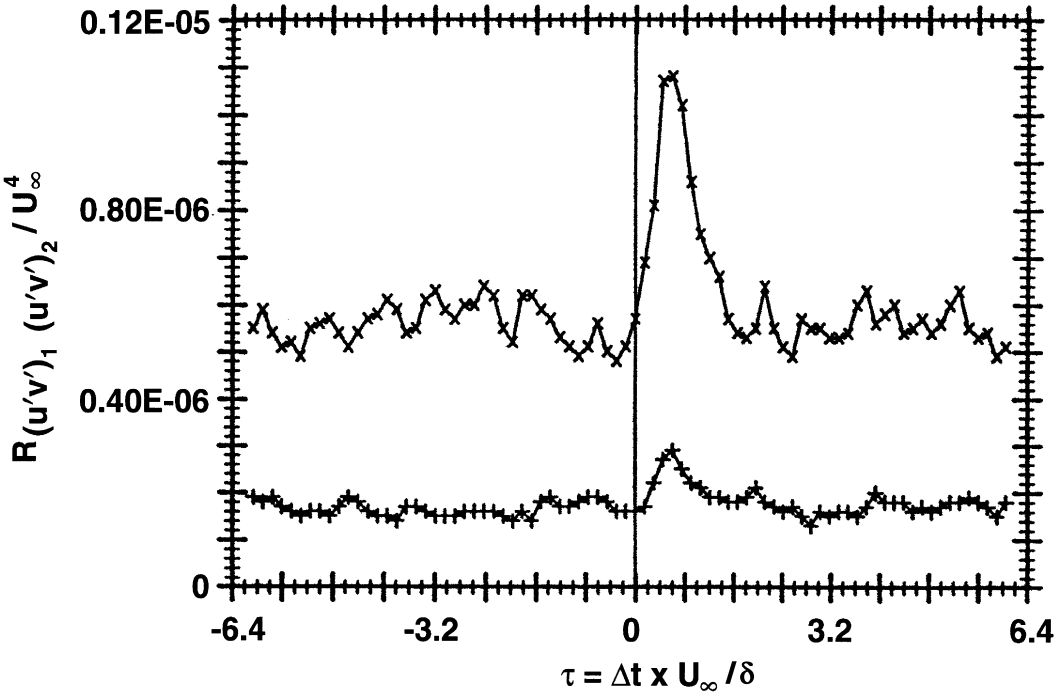

Fig. 11. Variation of $R_{(u'v')1}R_{(u'v')2}/U_\infty{}^4$ with τ for regular (x) and TAPPMed (+) boundary layers at $\xi = 20$.

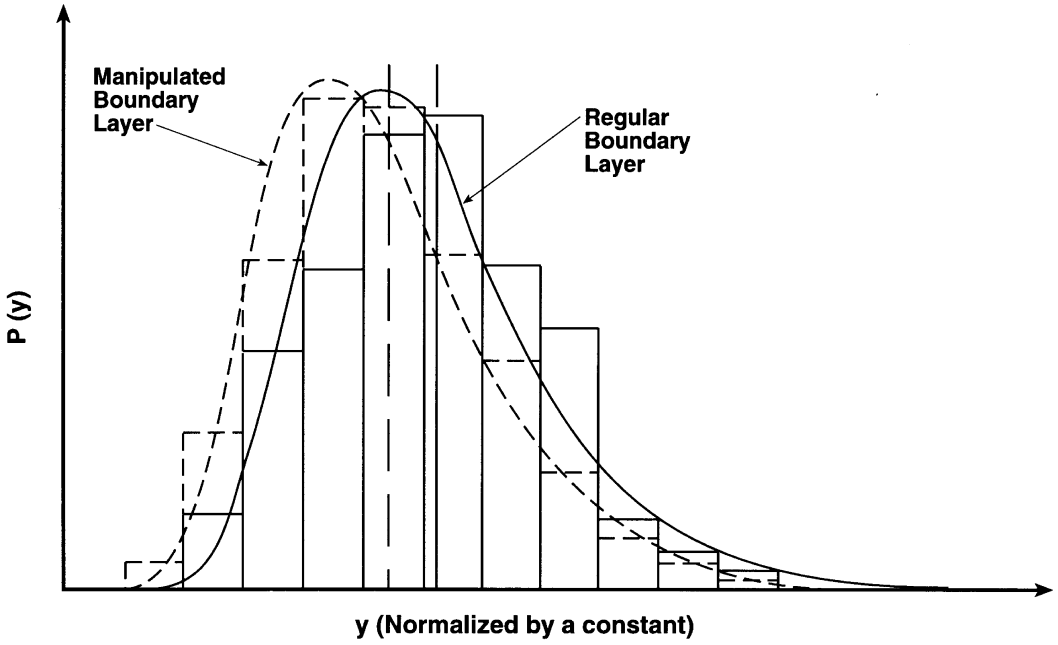

Fig. 12. Probability distribution of the position of a front of flow marker emanating from the wall $\pm 3.3\delta_o$ about $\xi = 20$, for the regular and TAPPMed boundary layers.

This reduced transport away from the wall is intimately associated with a reduction in the intensity of the bursting process in the region around $\xi = 20$.

The spread of the TAPPM wake were studied, using visualization technique, by laying a thin line of $TiCl_4$ on the upstream plate of the TAPPM. The spread of TAPPM wake was then photographed in a sheet of laser light. From several hundred pictures of this type we determined that the wake had remained remarkably intact, and had not spread to the wall region. To confirm that there was no interaction between wake vortices and the lifted wall layer fluid, we marked both the plate and the region of the wall discussed above. Figure 13 shows a representative picture of the wake that resulted, and the extent of the wall region eddies. Figure 13 also shows the spread of the wake of the upstream plate of the TAPPM, when the downstream plate has been removed. We can see that the wake has spread into the wall region and that there is considerably more interaction at the same streamwise location.

At $51\delta_o$, a distance of $31\delta_o$ farther downstream, the spatially separated temporal correlation measurements were repeated and are shown in Figs 14–17. It can be seen that all of the measures in the TAPPM modified flow are indistinguishable from those in the unmodified flow, with the exception of the correlation of the Reynolds stress, which has recovered approximately 80% of its unmodified value. Thus, the large scale motions have regained almost all of their strength over the $31\delta_o$.

The relaxation of the large scale motions was also observed using flow visualization, with contaminant introduced upstream of the boundary layer tip. Movies at $50\delta_o$ showed little perceivable change in the eddy structure (unlike the visualization of [21]). Examination of visualization of the spread of the wake from the first plate of the TAPPM (using the $TiCl_4$ visualization discussed above) showed that the wake spread across the boundary layer by approximately $50\delta_o$. Thus, there appears to be a correlation between the dispersion of the wake of the TAPPM across the boundary layer, and the relaxation of the LSMs and large scale irrotational flow. Furthermore, the skin friction, as measured by either method, has relaxed to a few percent of the unmanipulated value by this stage.

Measurements of the frequency of occurrence of the burst footprints (pockets, [8, 12]) at $51\delta_o$ showed that the number of pockets decreased by 11.6% when the TAPPM was present. When normalized on inner layer variables, u_τ and ν, there is only a 4% decrease in the number of pockets. When normalized on outer layer variables, a 21% decrease is found. Thus irrespective of which scaling is used, there are fewer pockets, and therefore fewer bursts of turbulence near the wall, consistent with reduced skin friction.

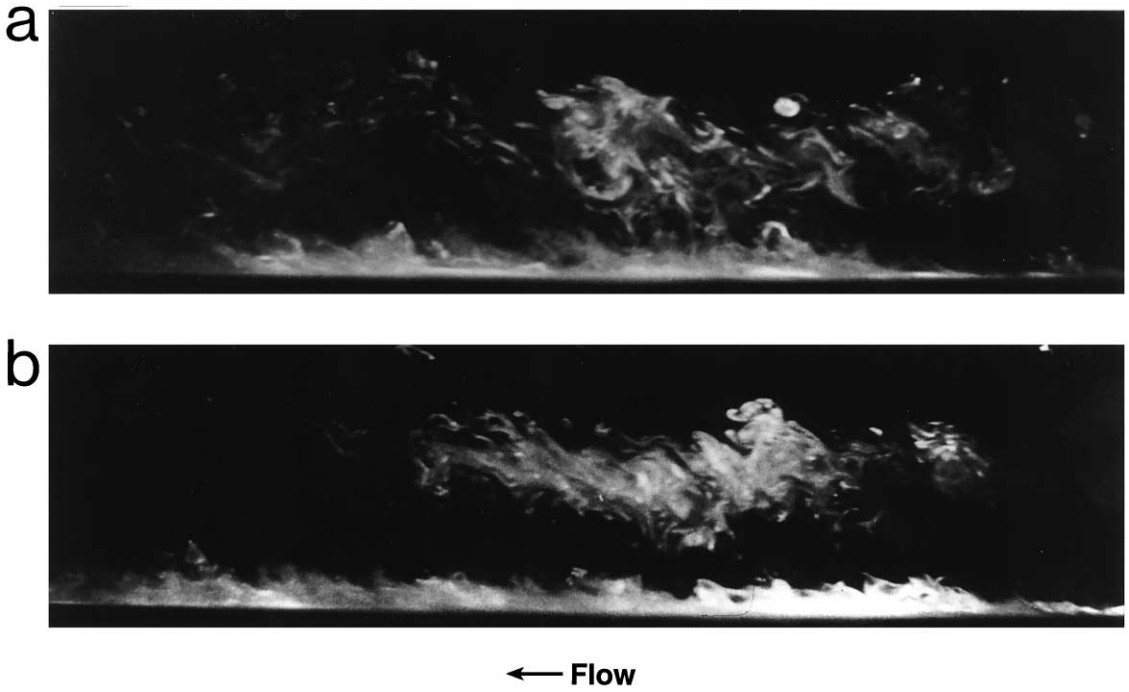

Fig. 13. Photos of the wakes of (a) the upstream plate by itself, (b) the TAPPM. Marker is also issuing from the wall. The center of the photos corresponds to $\xi = 20$.

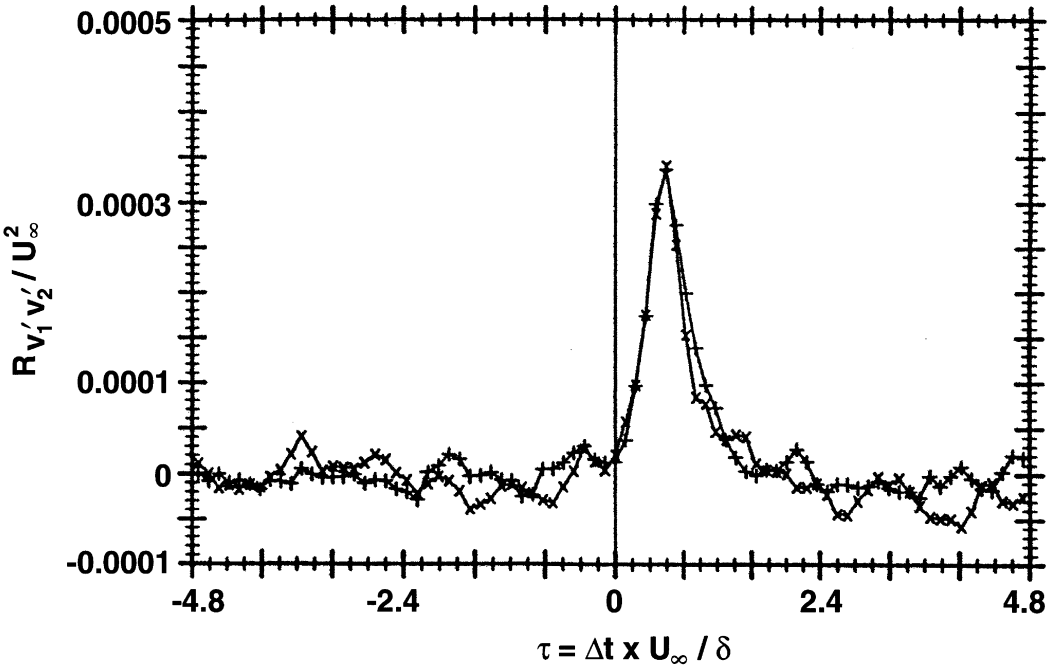

Fig. 14. Variation of $R_{v1'v2'}/U_\infty{}^2$ with τ for regular (x) and TAPPMed (+) boundary layers at $\xi = 51$.

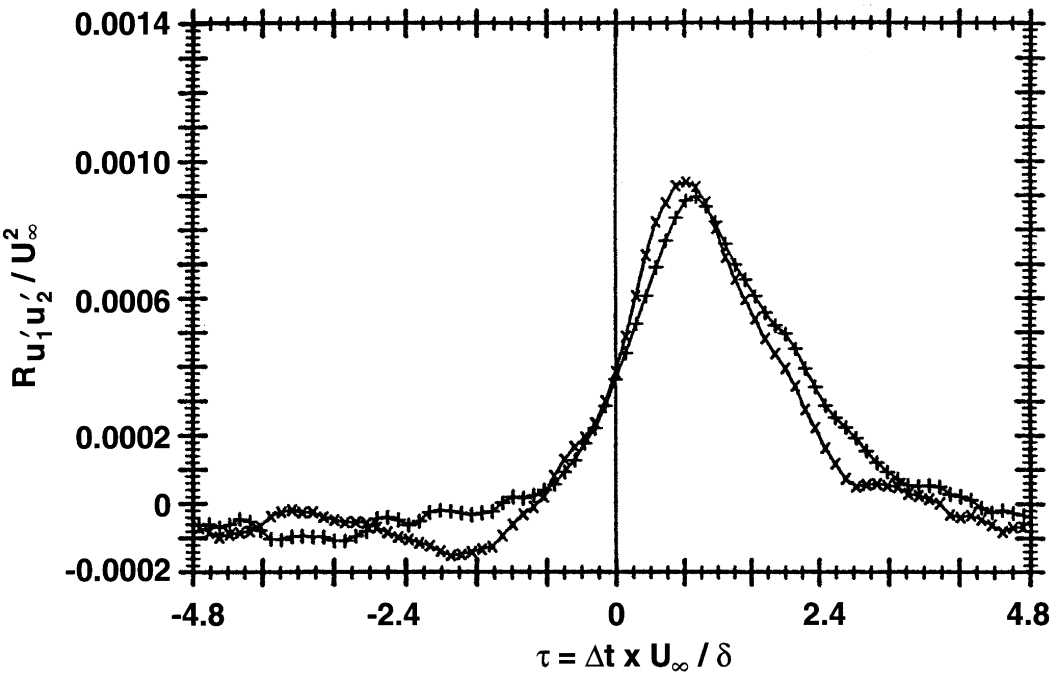

Fig. 15. Variation of $R_{u1'u2'}/U_\infty{}^2$ with τ for regular (x) and TAPPMed (+) boundary layers at $\xi = 51$.

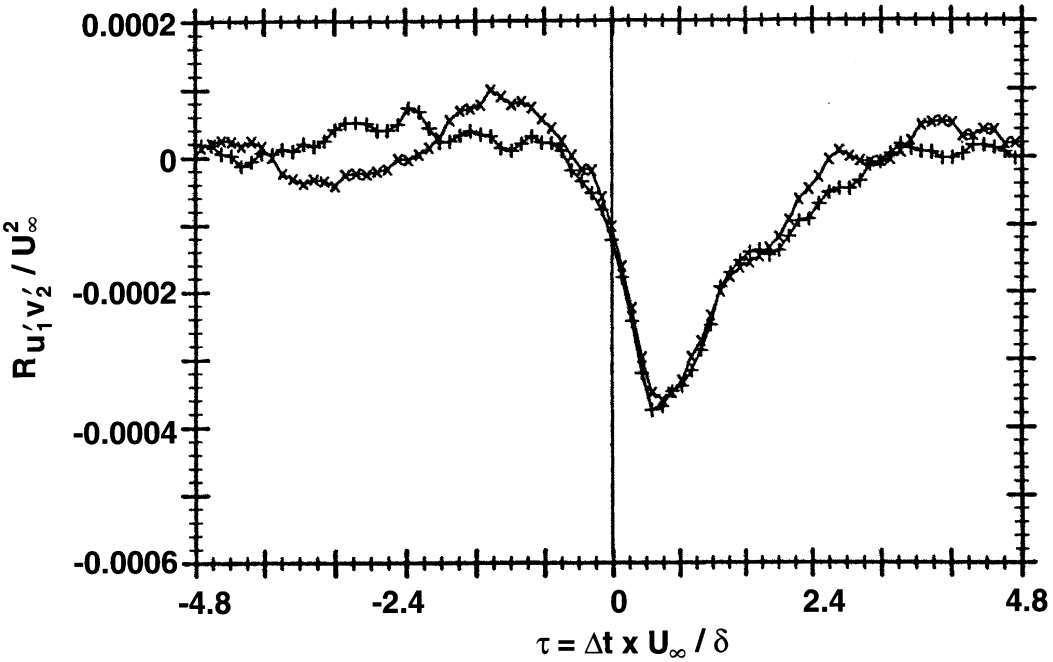

Fig. 16. Variation of $R_{u1'v2'}/U_\infty{}^2$ with τ for regular (x) and TAPPMed (+) boundary layers at $\xi = 51$.

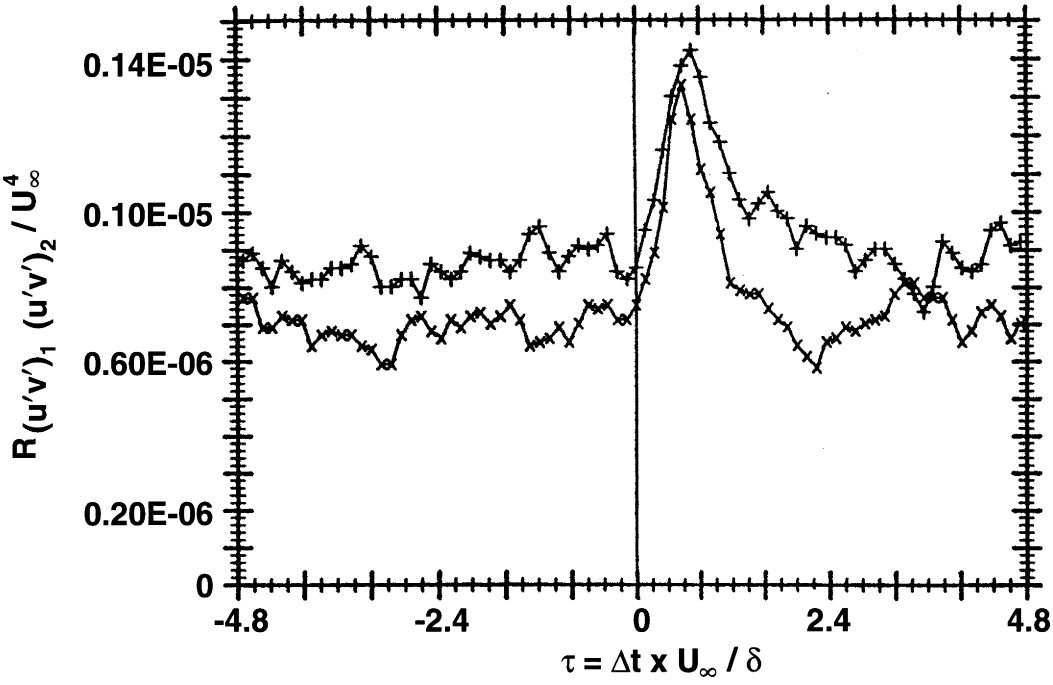

Fig. 17. Variation of $R_{(u'v')1}R_{(u'v')2}/U_\infty{}^4$ with τ for regular (x) and TAPPMed (+) boundary layers at $\xi = 51$.

It was possible to measure the thickness of the viscous sublayer by observing when the near-wall mean velocity profile data departed from linearity. Figure 18 shows the thickness for both TAPPM and regular cases. We found that the sublayer thickness increased by 15–20% over the range $20 < \xi < 95$. By $51\delta_o$ the large scale motions have relaxed back significantly, but both the burst rate and the sublayer thickness recover more slowly. This is consistent with a picture of the defect of the TAPPM's wake having spread to the wall region, and thereby being responsible for the remaining period of C_f reduction, after $51\delta_o$.

4. Discussion

Results show that the LSMs essentially recover at approximately the same distance from the TAPPM that the wake spreads across the boundary layer. This makes it difficult to cleanly separate out the various 'wake' effects, but simple arguments can show that 'plate' effects no longer are contributing to the C_f reduction.

4.1. Plate effects

At the plate, the streamwise component of the velocity is reduced to zero, and there is a reduction across the plate's boundary layers (whether laminar or turbulent), but no further away. Hence the net velocity defect in an LSM is increased by its passage through a plate. This increased defect will decrease as the wake spreads. In a uniform, irrotational ambient, our maximum wake defect would be reduced to 2% in $197\delta_o$, and have spread 5 cm. In our boundary layer, its defect was reduced to approximately 1% to 2% of U_∞ (estimated from the overall mean velocity profiles) at $20\delta_o$. No trace could be detected from the mean velocity profiles by $51\delta_o$, where observations showed that it appeared to spread across the boundary layer approximately 7.8 cm.

The vertical component also goes to zero at the plate, but the effect of the plate on 'v' inside and outside of the boundary layer is far reaching. Irrotational solutions combined with free streamline theory [22] suggest that the vertical component of velocity feels the plate a distance of approximately its length into the boundary layer and above it, which means that it is felt down to the wall. Combining the irrotational solution with a viscous solution near the plate, similar to [23], we see that the vertical component must decrease linearly as it approaches the plate outside of the plate's boundary layer. Thus 'v' is significantly affected across the flow, so that we should expect that $u'v'$ is significantly affected across the flow.

However, once the region of the flow has passed a plate, the effects of the plate on the normal component of velocity do not last as long as the streamwise velocity component effects. We can roughly estimate the number of boundary layer thicknesses over which we should expect it to reestablish itself. Since the relative defect has not changed, we certainly expect the flow around the

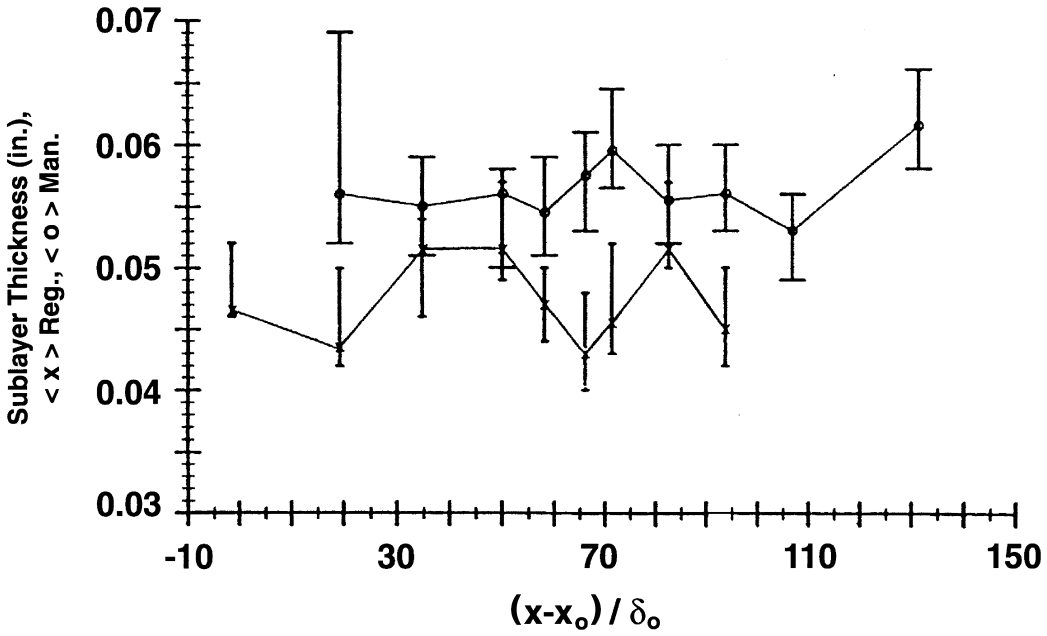

Fig. 18. Comparison of the sublayer thickness in regular (x) and manipulated (o) boundary layers. Limits of the error bars show the positions of the adjacent measurement positions for each profile.

LSMs will reestablish itself. Although the wake will result in both the eddies and the ambient moving with slower convection velocities, let us assume for estimation purposes that the convection velocity of the average LSM relative to the ambient remains at $0.8U_\infty$ [17], so for our flow, the oncoming stream requires 1/6 s to advance 1δ relative to the nearest downstream LSM. In this time the entire fluid has moved 5δ. After advancing this 5δ we would expect that the large scale wallward moving sweep would be fully reestablished. (Actually most valleys are less than δ in the streamwise direction, so this is a conservative estimate.) Inspection of Figs 6 and 8 shows that at $20\delta_o$ the 'v' component is far from being re-established, thus we expect that other mechanisms will be involved.

4.2. Wake effects

There are at least four different wake effects; shielding, unwinding, defect and wake/sublayer interactions. We feel that shielding is most strongly indicated by the data, and will present our argument for it in greatest detail.

4.2.1. Shielding

We suggest the reason the LSMs and their surrounding flow is not re-established quickly is due to the presence of the turbulent eddies in the wake of the TAPPM. The role of these eddies in the valleys is of particular significance as first suggested in [9]. The re-establishment of the large scale high energy flow around the LSMs is inhibited by the turbulence in this wake. The energy containing scales in the TAPPM's wake are the same order as the dissipative scales in the outer part of the boundary layer. This additional dissipative turbulence takes energy out of the freestream that would aid in re-establishing the large scale wallward sweeps. If it were not for the presence of the wake, the normal component, which is significantly affected by the 'plate' effect, would be re-established, and the Reynolds stress—in the valleys, at a minimum—would return to normal.

For the shield to develop it is important that the manipulator wake be allowed to develop. Wakes produced by devices too close to a wall can develop more as new boundary layers from rearward facing steps, and do not have the characteristic wake vortex structure.

Our results show that at $\xi = 20$, the wake from the TAPPM has not come within reach of the wall flow. We have, however, established approximately 40% C_f reduction based on the momentum balance estimates, and a 17% reduction based on the local C_f measurements. Thus, the mechanism of the interaction of the TAPPM's wake eddies with the sublayer [6] cannot be operative, and is apparently not responsible for these reductions. Our results showing the extent of marker spread away from the wall in this streamwise region, strongly support this conclusion. The remarkable coherence of the TAPPM wake in the region $\pm 3.3\delta$ around $\xi = 20$ further supports the wake shield hypothesis.

Further support for this hypothesis is the correspondence between the visual indication that the wake has spread across the layer by $51\delta_o$, and the data showing that the LSMs and the response of the irrotational ambient flow fields have re-established themselves at this location.

The studies of Eskinazi [24] also support our findings. Eskinazi studied the effects of a turbulent channel flow on the spread of a cylinder's wake and the effects of the wall on its spread. The cylinder diameter to the channel half width was 0.025. On average it was found that the wakes stayed intact, and spread slightly faster when developing in the surrounding turbulence; proportional to $x^{0.59}$ vs $x^{0.5}$. They had essentially the same velocity distribution as a wake in an initially uniform irrotational flow. Their presence increased the turbulence intensity across the wake-filled portion of the channel for the first ≈ 6 - $10\delta_o$; they did not follow the effects further. Corke [21] did, and showed that the intensity of a TAPPM first increased, then, by $\xi = 21$, had changed to being markedly lower on the wall side of the TAPPM, consistent with the results reported in [8].

It is interesting to note that shielding has the same effect as increasing the Reynolds number. Apart from the general effect of the wake's presence increasing the range of eddy scales in the spectrum, from a coherent structure point of view, at higher Reynolds numbers we find that the LSMs get closer together and the valleys are narrower, thus there is a less direct path for the high speed fluid to get down to the wall.

4.2.2. Unwinding

Photos just after the TAPPM show the wake roll-up into well defined eddies which alternately shed [8]. There is no correlation that can be obtained visually between the passage of the LSMs and the shedding of a particular sign of vorticity. Figure 6 indicates that the ensembled averaged peaks in the normal perturbation velocity are the order of 1% of U_∞. Thus, it appears that the perturbation in the circulation due to the passage of the LSMs is much weaker than that of the observed alternately shed TAPPM wake vortices, and would have correspondingly weaker effects on the LSMs.

4.2.3. Defect

It is clear that the average presence of lower momentum fluid near the wall will contribute to lower C_f and it is also clear that in each experiment sooner or later the wake intersects the wall. However, the arguments that the key mechanism being the TAPPM C_f reduction is simply the presence of lower momentum fluid in the boundary layer due to the defect of the TAPPM's wake [15], which is convected to the wall, thereby decreasing the wall shear, are open to two criticisms. First, as found

in this study, very high C_f reductions were found when the wake was more than its diameter away from the wall, and no indication of wake fluid could be seen in the wall region. Second, experiments with a cylinder versus a plate of equal momentum defect [6] indicated that the plate produced greater C_f reduction on the wall. It thus appears that defect is not necessarily the cause of peak reductions. However, the C_f reduction further downstream does not seem to be strongly affected by the type or height of the manipulator, and thus appears to result from the presence of the defect fluid from the wake intersecting the wall.

There is support for the role played by the wake's defect in producing the C_f vs ξ distribution when the wake has substantially intersected the wall at an early stage. Marumo et al. [25], using a much larger cylinder diameter to boundary layer thickness, 0.3, found that with the cylinder inside the layer at $y/\delta = 0.56$, a decrease in C_f resulted. In this case, the cylinder's wake half width intersected the wall within a few delta. This reduction appears to be due to the wake's defect. The turbulence intensities were generally higher whereas the local C_f was lower, opposite to the generally lower values found for lower drag plates and cylinders used as drag reducing manipulators.

4.2.4. The wake/wall interaction

Savill and Mumford [6] suggested that the reduction in skin friction observed in the region where they could visually observe the manipulator wake intersecting the wall, was due to "the lower wake vortices move down to the wall they induce a more vertical lift-up so C_f is further reduced ... Eventually the uplift is essentially vertical and virtually counters any local return flow, so we observe a general upward motion in the wall region and maximum skin friction reduction occurs". The results in [26] strongly suggests that the above description will result in increased C_f. In [26] it was found that a cylinder placed far enough away from a laminar boundary layer to allow its wake to properly form, produced a wake whose outermost vortices interacted with the boundary layer and caused it to undergo transition to a turbulent layer.

Figure 13 shows the situation $20\delta_o$ behind a single plate. It is an example of the situation we found when the wake has spread so its lower boundary is about a boundary layer microscale above the wall, and only its outermost parts are intersecting the wall. By the time this occurs, the kind of vortex organization referred to in [6] is totally gone, and the wake/wall interaction is further randomized because of the 'meandering' produced by the LSMs. We observed lift-up that is identical to those we observe when studying the bursting process in unmanipulated boundary layers [12, 26]. Each incursion from the wake represents a high Reynolds stress sweep which creates a pocket [12, 27], from which a lifted hairpin, called an ejection (also producing high Reynolds stress) emerges as observed in [6]. This process is highly three-dimensional and spatially random. This is hardly a region of reduced C_f brought about by a spatially uniform uplifting with unimportant weak return flow. We feel that this process strongly decreases the maximum C_f reductions that would otherwise be obtainable using TAPPMs.

Additional evidence supporting the picture was obtained in [25] for a much larger cylinder to boundary layer thickness, 0.3, where it was found that if the cylinder was just outside of the turbulent boundary layer, $h/\delta = 1.25$, the wall shear stress went up over the first $18\delta_o$, but decreased further downstream. With the wake outside of the boundary layer the effects appeared as free stream turbulence, for which both the skin friction and the turbulence intensities across the layer increased [28]. Excursions from the lower edge of the wake could reach the wall within a few delta, but the wake half width did not intersect the wall until about the streamwise position where C_f began to decrease below manipulated levels.

Choi [18] and Kovasznay et al. [19] have referred to the possibility that the presence of the wake in the logarithmic region would inhibit transport to the wall region, and called this 'blocking'. Careful differentiation needs to be made here. As the wake spreads into the log region it will certainly continue to inhibit the transport of the LSMs both towards and away from the wall, however with decreasing effectiveness, thus acting as inner region shield. But as indicated above, the lower extremities of the wake will interact with the sublayer and enhance the bursting process, which takes place on the scale of the wake's energy containing vortices (approximately the boundary layer microscale).

4.3. Bursting frequency

The results of the estimate of the frequency of occurrence of the bursting process from the pocket count at $51\delta_o$ has indicated that the number of pockets decreased. Depending upon the choice of scaling, the decrease ranged from 4 to 21%. Our $C_{f\theta}$ reduction was 40%, C_{fn}, C_{fp} and C_{fc} all about 5%. The decrease in the occurrence of the bursting process is consistent with reduced skin friction. Coughran and Bogard [30] found a decrease in the number of ejections, but using their scheme for deciding how many ejections correspond to a burst found an increasing number of bursts when scaled on inner layer variables. However, their wake appears to interact with the wall by $\xi = 27$, and their measurements are at $\xi = 24$ and 40. The wake in the present experiments interacts with the wall a little after our measurement position (starting at $56.5\delta_o$).

4.4. Further discussion and suggestions

It appears that the confusion with respect to the wake effects has resulted from the fact that experiments have been performed in boundary layers where the wake inter-

sected the wall over a range from 7 to $230\delta_o$, as estimated using the experimentally determined wake spread correlations for wakes in a turbulent ambient of [24]. Figure 19 shows the dependence of maximum net drag reduction and the minimum C_f on the distance downstream of the TAPPMs at which the wake half velocity thickness is one Taylor microscale away from the wall. Table 1 summarizes the parameters. We have included both local and integral techniques. On the whole, as the distance of the wake travels before interacting with the wall increases, so does the maximum C_f reduction, and the net drag reduction. Thus, the wake shield effect appears to be an important mechanism, and it is possible that some of the variation summarized in [2] is a result of having produced large variations in this mechanism.

Unfortunately when the wake eventually reaches the wall, we then have a period in which the lower wake vortices scour the wall, producing bursts of turbulence. This leads to a fairly rapid increase in the skin friction. This behavior of flow has been clearly observed in two different sets of measurements reported by Rashidnia [8–10]. Once the wake is substantially against the wall (the

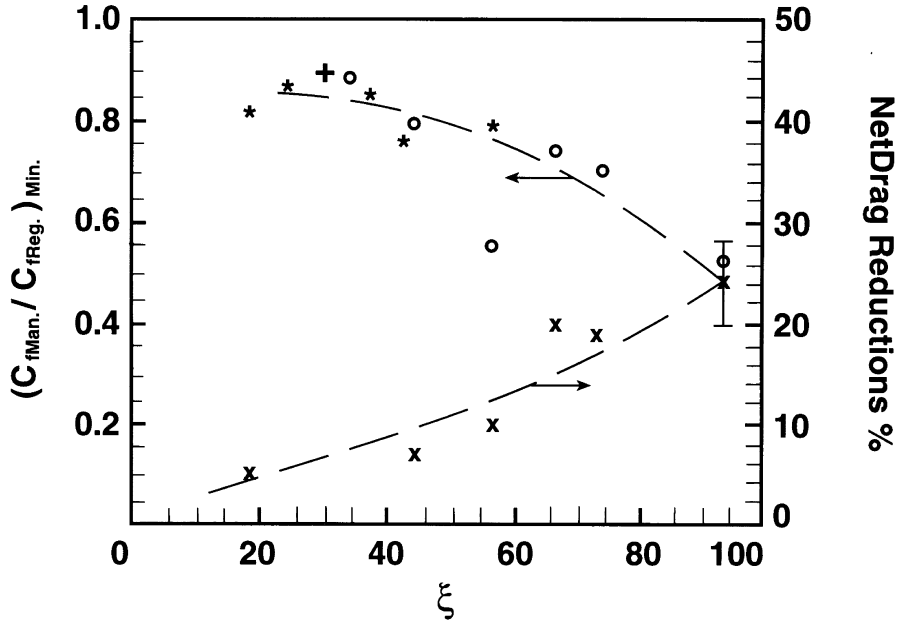

Fig. 19. Maximum net drag reduction, and maximum C_f reduction, as a function of the distance downstream from the TAPPM when the wake boundary is one microscale away from the wall: [x] Net drag reduction, [*] direct shear stress measurement, [o] momentum balance, and [+] Preston tube measurement.

Table 1
Maximum net drag and C_f reductions for TAPPMs

Source	From trailing edge of TAPPM	Momentum balance	Preston tube	Direct measurement	Percent net drag reduction
[15]	18.8			0.82	5
[5]	24.6			0.86	
[30]	34.2	0.88			
[33]	37.4			0.85	
[32]	42.6			0.76	
[1]	44.2				7
[8]	56.5	0.55	0.89	0.79	10
[21]	66.4	0.735			20
[3]	73.9	0.70			5
[7, 14]	93.9	0.52			20–28

half velocity thickness has intersected) the remaining wake defect sustains an approximately 5% C_f reduction for a considerable distance before it is completely mixed.

Using the above picture, we can explain the change in the shape of C_f with distance and the changes in this distribution with h/δ_o. The peak in C_f reduction observed when the TAPPM is in the layer, is associated with the influence of the wake on the LSMs. When a TAPPM is above δ_o, its influence resembles that of free stream turbulence on the boundary layer [25]. It has little 'plate' influence on the LSMs and has high speed fluid between it and the boundary layer to supply the normal amounts of energy. As a manipulator is moved to the edge of the layer, a number of the largest LSMs are affected by it. By $h/\delta_o = 1$, both 'plate' and wake shielding effects can manifest themselves, so we see a decrease in C_f. Because the wake is only partially interfered with by the turbulence, its spread rate remains small, and thus, its effects are approximately uniform over a considerable streamwise distance ($\xi \approx 150$–200). As the manipulator is moved further into the boundary layer, the majority of LSMs are affected by it, as is the irrotational fluid that responds to them. Thus, as we move downstream from the manipulator, we see a rapidly increasing effect—with time scales appropriate to the microscale eddies (λ) of the outer region—as more of the large scale wallward moving fluid is disrupted from its path towards the wall. Thus, we should not see an immediate reduction in the wall shear stress due to this effect. Estimating the time scale by $t = \lambda/(\text{rms } u')$, the flow will convect tU_∞ before appreciable changes occur. For our Reynolds number, $\lambda \approx 0.15\delta_o$, and an average intensity rms u'/U_∞ of 2%, thus, the flow will convect $\approx 7\delta_o$. All data show that approximately this distance is required before appreciable reductions are found with TAPPMs at 0.75–$0.8\delta_o$. About $25\delta_o$ the peak reductions occur. All the time the wake is spreading according to $x^{0.59}$. When it nears the wall, it will have the effect of increasing the C_f as indicated above. This accelerates the spread of the wall side of the wake, and it rapidly is brought to the wall. Once this occurs, the velocity gradients at the wall will diminish, and the C_f will not rise further, until the wake defect has thoroughly mixed.

We have found that the wake shielding effect is likely to be of significant help in sustaining the C_f decrease, while the wake/wall region interaction effects acts to increase C_f. We believe that the wake shielding effect complements the plate effect, and that both are needed to attain net drag reduction using TAPPMs. Although there is a rise in C_f when the wake approaches the wall, this is reduced in intensity because of the thickened sublayer that develops. Chu [31] showed that the eddies initiating the bursting process resulted in weaker interactions when the sublayer is thicker. Thus, we want to delay the interaction of the wake with the sublayer as long as possible. Experiments with cylinders appear to support this point of view [6, 32]. Simply putting a wake of the same defect into the flow, without first decreasing the strength of the turbulence by the plate effects, will result in the wake being spread more rapidly (at $x^{0.59}$), and thus losing its effect before the device drag has been recovered. Extrapolation to thicker layers and other Reynolds numbers needs to be done considering the desire for the wake to produce eddies in the dissipation range. It is clear that as δ increases, the minimum plate thickness required for and optimum shield will increase.

In Figure 13, as well as noted above, flow visualization showed that the wake of one plate spread much faster than that of the TAPPM. Since we have argued that maintaining the coherence of the wake in the outer part of the boundary layer is key to the shielding effect, we believe that TAPPMs work better than single plates of the same total chord—in spite of the drag penalty—because their wake spreads less. The reason for this reduced spreading rate are, however, not clear.

To optimize the wake shielding effect, we need to understand how to keep a wake from spreading as rapidly. This may appear difficult, but TAPPMs are certainly one way, and understanding how they accomplish this may lead to others. Further testing of the wake shielding model will have to be made in thicker boundary layers than generally used, as lower defect wakes are difficult to produce with passive devices.

5. Conclusions

A TAPPM was used to produce a flow with net drag reduction. Conditionally sampled measurements show that the LSMs are significantly changed at $20\delta_o$ and that the flow fields in the 'valleys' are equally affected. Both the turbulent and irrotational flows then re-establish themselves for—all practical purposes by $50\delta_o$. The skin friction begins to rise before this because of the wake/wall turbulence amplification effect. Arguments indicate that the effects of the TAPPM on the large scale sweeps produced by the velocity defect of the large eddies should be removed by 5δ. Visualization showed that the TAPPM wake was very coherent at $20\delta_o$, and had not spread into the wall region. The fact that the LSMs and the ambient response flow continue to show strong changes at $20\delta_o$ and beyond, supports a picture in which the shielding effect of the wake of the TAPPM acts to prolong the suppression of the large scale motions, and thereby is an essential part of the mechanism by which the manipulator reduces the skin friction over a sufficiently long extent of the boundary layer, so as to overcome the device drag and result in a net drag reduction. In thicker boundary layers it is expected that the shielding effect will become an increasingly important part of the overall picture. Extrapolation suggests that there may be lower limits

on the thickness of TAPPMs that will produce effective shields.

Acknowledgements

We would like to thank Dr Falco for his advice and continuous support throughout this project carried out at the Turbulence Structures Laboratory at Michigan State University. These experiments were performed with the aid of financial support from NASA grant NAG-1-302. Analysis was performed with support from AFOSR grant 87-0047.

References

[1] J.B. Anders, J.N. Hefner, D.M. Bushnell, AIAA Paper 84-0345 1984.
[2] J.B. Anders, AIAA Inc., New York, 123 (1990) 263–284.
[3] E. Coustola, A.M. Savill, AGARD Report 786 (1992) pp. 55–80.
[4] G. Iuso, The Aeronautical Journal 98 (980) (1994).
[5] J. Lemay, D. Provenacal, R. Gourdeau, V. D. Nguyen, J. Dickinson, AIAA Paper 85-0521, 1985.
[6] A.M. Savill, J.C. Mumford, J. Fluid Mech. 191 (1988) 389–418.
[7] M.W. Plesniak, H.M. Nagib, AIAA Paper 85-0518, 1985.
[8] N. Rashidnia, Ph.D. thesis, Department of Mechanical Engineering, Michigan State University, 1985.
[9] N. Rashidnia, R.E. Falco, Bull. Am. Phy. Soc. Series II 32 (10) (1987) 2088.
[10] N. Rashidnia, R.E. Falco, Bull. Am. Phy. Soc. Series II 30,(1985) 1711.
[11] G. Iuso, M. Onorato, Meccanica 4, (1995) 1–17.
[12] R.E. Falco, AIAA Paper 83-0377, 1983.
[13] K.R. Sreenivasan, R. Narasimha, AIAA Paper 85-0518 1985.
[14] Y.G. Guezennec, H.M. Nagib, AIAA Paper 85-0519, 1985.
[15] S. Taylor, Ph.D. thesis, GALCIT Cal. Tech., 1986.
[16] D.M. Bushnell, AIAA Paper 83-0227, 1983.
[17] A.P. Dowling, Internal Report, Cambridge University Engineering Department, 1984.
[18] K. Choi, NMI Report R193 1984.
[19] L.S.G. Kovasznay, V. Kibens, R.F. Blackwelder, J. Fluid Mech. 41 (1970) 283–387.
[20] S.P. Govindaraju, F.W. Chambers, AIAA J. 25 (1987), 388–394.
[21] T.C. Corke, Ph.D. thesis, Illinois Institute of Technology, Chicago, Illinois, 1981.
[22] L.M. Milne-Thomson, Theoretical Hydrodynamics, 4th ed., MacMillan, New York, 1960.
[23] H. Schlichting, Boundary Layer Theory, McGraw-Hill, New York, 1979.
[24] S. Eskinazi, NASA TN D-83, 1959.
[25] E. Marumo, K. Suzuki, T. Sato, J. Fluid Mech. 87, (1978) 121–141.
[26] R.E. Falco, in: C.R. Smith, D.E. Abbott (Eds.), Coherent Structure of Turbulent Boundary Layer, AFSOR/Lehigh, 1978, pp. 448–461.
[27] R.E. Falco, AIAA Paper 80–1356, 1980.
[28] G. Charnay, Ph.D. thesis, University Claude Bernard, Lyon , 1974.
[29] A.M. Savill, Euromech 181, Saltsjobaden, Sweden, 1984.
[30] M.T. Coughran, D.G. Bogard, Proceedings of the Tenth Symposium on Turbulence, Rolla, Mo., 22–24 September, 1986.
[31] C.C. Chu, Ph.D. thesis, Department of Mechanical Engineering, Michigan State University, 1987.
[32] T.B. Lynn, K.R. Sreenivasan, Yale University Report, 85 FM 2, 1985.
[33] R.V. Westphal, AIAA Paper 86-0283, 1986.